



## CONTRIBUTED ARTICLE

# Dynamics of a Random Neural Network with Synaptic Depression

W. SENN,<sup>1</sup> K. WYLER,<sup>1</sup> J. STREIT,<sup>2</sup> M. LARKUM,<sup>2</sup> H.-R. LÜSCHER,<sup>2</sup> H. MEY,<sup>3</sup> L. MÜLLER,<sup>1,3</sup>  
D. STAINHAUSER,<sup>1</sup> K. VOGT<sup>2</sup> AND TH. WANNIER<sup>2</sup>

<sup>1</sup> Institut für Informatik und angewandte Mathematik, Universität Bern, <sup>2</sup> Physiologisches Institut, Universität Bern, and  
<sup>3</sup> Ascom Tech AG

(Received 13 December 1994; accepted 12 July 1995)

**Abstract**—We consider a randomly connected neural network with linear threshold elements which update in discrete time steps. The two main features of the network are: (1) equally distributed and purely excitatory connections and (2) synaptic depression after repetitive firing. We focus on the time evolution of the expected network activity. The four types of qualitative behavior are investigated: singular excitation, convergence to a constant activity, oscillation, and chaos. Their occurrence is discussed as a function of the average number of connections and the synaptic depression time. Our model relies on experiments with a slice culture of disinhibited embryonic rat spinal cord. The dynamics of these networks essentially depends on the following characteristics: the low non-structured connectivity, the high synaptic depression time and the large EPSP with respect to the threshold value. Copyright © 1996 Elsevier Science Ltd

**Keywords**—Random neural network, Threshold element, Synaptic depression, Average activity, Dynamics, Oscillation, Disinhibited connections, Embryonic spinal cord.

## 1. INTRODUCTION

Artificial neural networks designed as models to understand the functioning of biological networks are usually based on experimental data from adult or at least postnatal animals. Such networks consist of highly structured excitatory and inhibitory synaptic connections, a high degree of convergence and divergence with corresponding low weights of single unit connections and thus of neurons with a manifold repertoire of integrative properties and a wide range of frequencies of output patterns. The analysis of such networks is usually task-oriented. That is, its artificial model is designed to perform the same task as the biological network is believed to do. The disadvantage of such an approach is that a certain biological task may be performed by a variety of differently structured networks and therefore a

simple analogy can not be conclusive concerning the actual biological mechanism. In other words it is questionable whether the structure of a network is strictly determined by its function. More probably, an additional dimension has to be considered in order to understand a network's structure and this is its developmental history. During development the properties of neurons and neuronal networks undergo dramatic changes: embryonic networks often lack functional inhibitory contacts (Oppenheim, 1975). The degree of convergence and divergence is low with corresponding high weights of single unit connections (Streit et al., 1991) and consequently the integrative properties of the neurons are of low importance. In addition, the range of output frequencies of neurons is strongly limited by the poor frequency response of impulse conduction and synaptic transmission. In consequence, synaptic efficacy rapidly decreases at frequencies above 1 Hz (Streit et al., 1992).

In order to learn something about the possibilities of activity-dependent self-organization of embryonic networks during periods of spontaneous activity, the dynamics of randomly connected networks with high individual weights, a low degree of connectivity and

---

Acknowledgement: This work was supported by the Swiss National Science Foundation (NFP/SPP grant No. 5002-03793).

Requests for reprints should be sent to Walter Senn, Institut für Informatik und angewandte Mathematik, Universität Bern, Neubrückestrasse 10, CH-3012 Bern, Switzerland.

strong synaptic depression were analyzed for their capability of providing a stable oscillatory output. Such networks with a stable oscillatory output based on endogenous properties were described in a rat spinal cord culture system (Streit, 1993), and are believed to be involved in the formation of spinal pattern generators for locomotion (Grillner, 1985; O'Donovan et al., 1992). It is shown that stable oscillations of activity can arise in such networks simply as a result of the endogenous properties mentioned above regardless of the particular network structure. Furthermore the patterns of activity can be altered by changing single parameters like the average synaptic weight or the mean rate of connectivity.

The dynamics of a homogeneous random network similar to ours was first investigated theoretically by Amari (1971). In contrast to his work we consider in addition the synaptic depression after firing. In typical time-discrete random networks the synaptic depression is modeled by an absolute refractory period lying between once and twice the interneural delay, see for example, Anninos et al. (1970) and Fournou et al. (1993). However, this is a very strong restriction. In our approach an arbitrary synaptic depression time is allowed and we have a continuous regeneration of the synaptic efficacy. Oscillations of an excitatory network with interneural delays and phenomenologically described neurons were investigated by J.-F. Vibert and recently appeared in this journal (Vibert et al., 1994). Although we do not consider such delays, the various patterns of network activity as oscillations, chaos or constant activity can be explained. With appropriate modifications to the neuron model we are able to give some rigorous mathematical statements on the long-term behavior of network activity. We pick up Vibert's question of whether rhythmic patterns rely on pacemaker cells or whether they are an emerging property of the network (Vibert et al., 1994, p. 589). In the case of the embryonic networks, our results suggest that oscillations indeed originate from the typical range of parameter values measured in the slice cultures of embryonic rat spinal cord. In particular, pacemaker cells seem not to be necessary.

The paper is organized as follows: Section 2 states the mathematical model together with the biological assumptions. Two versions of the synaptic depression are modeled. In the first case, synaptic depression is excluded making it possible to classify the networks according to the long-term development of the average activity (Section 3). In Section 4, we include the synaptic depression and discuss the activity as a function of the average number of connections and the synaptic depression time. Finally, in Section 5, some physiological conclusions are drawn from the preceding mathematical analysis.

## 2. THE MODEL OF A HOMOGENEOUS RANDOM NETWORK

### 2.1. Assumptions about the Network

We consider a purely excitatory random network with neurons being linear threshold elements. The (excitatory) connections between the neurons are subject to synaptic depression. Time is considered to be discrete. A neuron receives possibly depressed excitatory post-synaptic potentials (EPSPs) at time  $t$  if it has input-connections from cells which are active at the same time  $t$ . The neuron will itself be active at time  $t + 1$  if the sum of incoming EPSPs at time  $t$  exceeds a fixed threshold value  $\theta > 0$ . Due to the short decay time of the soma potential, for any neuron the potential is reset to 0 (corresponding to about  $-60$  mV in an absolute scale) at the beginning of the next time step  $t + 2$ . This reset is reasonable if we assume that the time between two succeeding time steps  $t$  and  $t + 1$  in our discrete model corresponds to 14 ms in nature. This time of 14 ms is the mean value of the measured conduction delays between two cells in the slice culture of embryonic rat spinal cord (Streit et al., 1991).

The two main characteristics of the network are:

1. *The Poisson Distribution of the Connections.* Let the network consist of  $N$  neurons and let us suppose that the connections of a single neuron to the  $N$  cells are uniformly distributed in space. The number of such connections is assumed to be Poisson distributed with mean  $\mu$ . Thus, the probability for a neuron to have  $m$  output-connections is

$$p_m = \frac{\mu^m}{m!} e^{-\mu}.$$

Conversely, due to the uniform distribution, the number of connections a neuron receives from other cells is given by the same distribution  $p_m$ .

2. *The Synaptic Depression after Firing.* Let the undepressed post-synaptic potential induced by a single action potential of a pre-synaptic cell be denoted by  $K > 0$ . Thus,  $K$  corresponds to the maximal increase of the post-synaptic membrane potential if one of the  $\approx \mu$  connections to a cell is activated. (The undepressed post-synaptic potential  $K$  itself may be composed of multiple *unitary* EPSPs, which, however, we do not consider. If a neuron had fired exactly once already, say at time interval  $\Delta t$  before the present time  $t$ , the EPSP it might produce at the present time  $t$  is depressed by a factor  $(1 - e^{-\Delta t/\tau})$ . The constant  $\tau > 0$  is called the *synaptic depression time*. Thus, the effective EPSP the neuron may produce at time  $t$  with one

single output-connection is  $K \cdot (1 - e^{-\Delta t/\tau})$ . If the neuron fired in addition  $\Delta t' \neq \Delta t$  time-intervals before the present time  $t$ , this EPSP is depressed once more to the value  $K \cdot (1 - e^{-\Delta t/\tau}) (1 - e^{-\Delta t'/\tau})$ . The factor by which the original EPSP of height  $K$  is depressed will be called the *synaptic efficacy* of the neuron. A neuron will reach its lowest synaptic efficacy if it fires every time step  $1, 2, 3, \dots$ . In this case, its synaptic efficacy at time  $t$  is  $(1 - e^{-1/\tau}) \cdot \dots \cdot (1 - e^{-t/\tau})$ . Although this expression decreases monotonically with increasing  $t$ , the synaptic efficacy is shown to be always larger than a fixed positive constant (Lemma 1).

**2.2. Deduction of the Macroscopic State Equations**

The macroscopic state of the network at time  $t$  is characterized by two variables: the *average activity*  $a_t$  and the *average synaptic efficacy*  $s_t$ . The average activity is defined by

$$a_t \doteq \frac{1}{N} \sum_{i=1}^N a_t^i,$$

where  $a_t^i$  is 1 or 0 if the  $i$ th neuron at time  $t$  is active or not, respectively. The average synaptic efficacy is given by

$$s_t \doteq \frac{1}{N} \sum_{i=1}^N s_t^i,$$

where

$$s_t^i \doteq (1 - a_{t-1}^i e^{-1/\tau}) \cdot (1 - a_{t-2}^i e^{-2/\tau}) \cdot \dots \cdot (1 - a_0^i e^{-t/\tau})$$

is by definition the synaptic efficacy of the  $i$ th neuron.

Let us calculate the expectation values of  $a_{t+1}$  and  $s_{t+1}$  if the average activities up to time  $t$  are given. First, we show that the expectation value of  $s_{t+1}$  takes the form

$$\langle s_{t+1} \rangle = (1 - a_t e^{-1/\tau}) \cdot (1 - a_{t-1} e^{-2/\tau}) \cdot \dots \cdot (1 - a_0 e^{-(t+1)/\tau}). \quad (1)$$

By the law of large numbers,  $a_t$  may be identified by the probability that an arbitrary neuron gets excited at time  $t$ . The expectation value  $\langle s_{t+1}^i \rangle$  for any cell  $i$  therefore is equal to the right-hand side of (1). Since this value is independent of  $i$ , the expectation value  $\langle s_{t+1} \rangle$  of the average synaptic efficacy is the same as the expectation value  $\langle s_{t+1}^i \rangle$  for a single neuron. This proves (1).

The expectation value  $\langle a_{t+1} \rangle$  is obtained analogously by calculating first  $\langle a_{t+1}^i \rangle$ . By assumption, the

probability for neuron  $i$  of having  $m$  input-connections is given by the Poisson density  $p_m$  with mean  $\mu$ . Since the connections are uniformly distributed on each subset of neurons, the number of connections from the subset of *active* neurons to neuron  $i$  is again Poisson distributed, now with mean  $a_t \mu$ . Thus, the probability of having  $m$  input-connections from active cells is

$$\frac{(a_t \mu)^m}{m!} e^{-a_t \mu}.$$

Let the threshold  $\theta$  be normalized to  $\theta = 1$ . Since the average EPSP the neuron  $i$  receives is  $Ks_t$ , it needs at least

$$\eta_t \doteq \left[ \frac{1}{Ks_t} \right]^+$$

EPSPs to get excited. By  $[x]^+$  we denote the smallest integer  $\geq x$ . Thus, the probability of neuron  $i$  becoming excited is given by the sum of all

$$\frac{(a_t \mu)^m}{m!} e^{-a_t \mu}$$

with  $m \geq \eta_t$ . Again, this does not depend on  $i$  and we get the expectation value of the average  $a_t$  as

$$\begin{aligned} \langle a_{t+1} \rangle &= \langle a_{t+1}^i \rangle = \sum_{m=\eta_t}^{\infty} \frac{(a_t \mu)^m}{m!} e^{-a_t \mu} \\ &= 1 - e^{-a_t \mu} \sum_{m=0}^{\eta_t-1} \frac{(a_t \mu)^m}{m!}. \end{aligned} \quad (2)$$

If we want to predict the macroscopic state  $a_t$  and  $s_t$  a certain number of time steps in advance we are forced to approximate them by their expectation values  $\langle a_t \rangle$  and  $\langle s_t \rangle$ , respectively. The macroscopic state equations we obtain with this approximation from (1) and (2) are

$$\begin{aligned} a_{t+1} &= 1 - e^{-a_t \mu} \sum_{m=0}^{\eta_t-1} \frac{(a_t \mu)^m}{m!}, \quad \eta_t = \left[ \frac{1}{Ks_t} \right]^+ \\ s_{t+1} &= \prod_{i'=0}^t (1 - a_{t-i'} e^{-i'+1/\tau}). \end{aligned} \quad (3)$$

Applying the Chebyshev inequality we can estimate the error of this approximation: since  $a_t$  and  $s_t$  are weighted sums of the identically distributed random variables  $a_t^i$  and  $s_t^i$  ( $1 \leq i \leq N$ ), respectively, each lying between 0 and 1, the standard deviation of  $a_t$  and  $s_t$  may be uniformly estimated by  $\text{const } 1/\sqrt{N}$ . In other words, the error from (2) to (3) is of order

$$\langle a_{t+1} \rangle - a_t = O\left(\frac{1}{\sqrt{N}}\right)$$

independently of  $t$ . Iterating (2) and (3) separately  $\Delta t$  times, this error is growing with  $\sqrt{\Delta t}$ . The reason is the same as for symmetric random walks, here with step-length  $1/\sqrt{N}$ : if the error  $1/\sqrt{N}$  has sign + or - with equal probability, the expected error after  $\Delta t$  iterations is of order  $\sqrt{\Delta t}/\sqrt{N}$  (this again is essentially due to the Chebyshev inequality). Therefore, a prediction of  $a_t$  for  $\Delta t$  time steps in advance is reasonable only if the number  $N$  of neurons in the network exceeds itself the order of  $\Delta t$ .

To end, let us state the soothing fact that the average synaptic efficacy  $s_t$  will never converge to 0.

**LEMMA 1.** *For any  $t \in N$  and any  $a_{t-t'} \in [0, 1]$ ,  $t' \leq t$ , the synaptic efficacy is bounded from below by the inequality*

$$s_{t+1} = \prod_{t'=0}^t (1 - a_{t-t'} e^{-(t'+1)/\tau}) \geq e^{-\tau \pi^2/6}.$$

*Proof.* Replacing  $a_{t-t'}$  by 1 yields

$$\begin{aligned} -\log s_{t+1} &\leq -\sum_{t'=0}^t \log(1 - e^{-(t'+1)/\tau}) \leq \\ &-\int_0^\infty \log(1 - e^{-t'/\tau}) dt' \\ &= \tau \int_{-1}^0 \frac{\log(x+1)}{x} dx \\ &= \tau \left(1 + \frac{1}{2^2} + \frac{1}{3^2} + \dots\right) = \tau \frac{\pi^2}{6}. \quad \square \end{aligned}$$

### 2.3 Modification of the model

In order to make the state equations more accessible to analysis, we need some modifications.

First, we replace the integer

$$\eta_t = \left\lceil \frac{1}{Ks_t} \right\rceil^+$$

by the quantity  $1/Ks_t$  which is differentiable in  $K$  and  $s_t$ . Since we are dealing with mean values, this replacement is reasonable. To adapt the formula of  $a_{t+1}$  for real values of  $\eta_t$  we rewrite it as a Gamma distribution function

$$1 - e^{-a_t \mu} \sum_{m=0}^{\eta_t-1} \frac{(a_t \mu)^m}{m!} = \frac{1}{\Gamma(\eta_t)} \int_0^{\mu a_t} x^{\eta_t-1} e^{-x} dx, \quad \eta_t \in N.$$

The equality is derived by integrating partially  $(\eta_t - 1)$  times. While the left-hand side makes sense only for  $\eta_t \in N$ , the right-hand side now may be evaluated for any  $\eta_t \in R^+$ .

Second, we give a variant of the synaptic efficacy.

Instead of the synaptic efficacy we interpret  $s_t$  as a (average) *synaptic reliability*: we assume that a synapse transmits the whole undamped potential  $K$  with probability  $s_t$  while it fails to work with the counter probability  $1 - s_t$ . Consequently, the probability that an EPSP of height  $K$  is coming in by a single input-connection is given by  $a_t s_t$ . With this interpretation of  $s_t$  as synaptic reliability, the activity at time  $t + 1$  will be calculated by

$$a_{t+1} = \frac{1}{\Gamma\left(\frac{1}{K}\right)} \int_0^{\mu a_t s_t} x^{1/K-1} e^{-x} dx.$$

The interpretations of  $s_t$  as synaptic efficacy and synaptic reliability tend to be equivalent, if the average number  $\mu$  of input-connections of a neuron is large: in both cases, the average activity of the neurons is the same since the expectation value for the summed EPSPs one neuron receives at time  $t + 1$  is the same: it is  $\mu(Ks_t)a_t$  in the case of synaptic efficacy and  $\mu K(s_t a_t)$  in the case of synaptic reliability. While the expectation of the summed EPSPs one neuron receives is the same, its standard deviation differs in the two interpretations. If  $\mu$  is large, however, the deviation converges to 0 in both cases. Indeed, for large  $\mu$  the summed EPSP is Gaussian distributed around its expectation value according to the central limit theorem. Its standard deviation is  $Ks_t \sqrt{\mu a_t (1 - a_t)}$  in the case of synaptic efficacy and  $K \sqrt{\mu a_t s_t (1 - a_t s_t)}$  in the case of synaptic reliability. Since from a biological point of view it is reasonable to require that  $\mu K$  is bounded (say of order  $10 \cdot \theta$ ), both these deviations tend to 0 with growing  $\mu$ . These arguments show that, for a large number  $\mu$  of connections, the average activity  $a_t$  of the neurons indeed does not change essentially if, instead of the synaptic efficacy, we consider the synaptic reliability.

Third, we reduce the dynamics of model (3) to a two-dimensional Markov process. For this we have to suppress the explicit influence of the past activities  $a_{t-1}, a_{t-2}, \dots$  in the formula for  $s_{t+1}$ . Since the influence of  $a_{t'}$  on  $s_{t+1}$  decays with growing time-distance  $t - t'$  the second-order approximation of  $s_{t+1}$  is given by

$$s_{t+1} \approx (1 - a_t e^{-1/\tau})(1 - a_{t-1} e^{-2/\tau}). \quad (4)$$

In order to obtain a mapping  $(a_t, s_t) \rightarrow (a_{t+1}, s_{t+1})$  we calculate the activity  $a_{t-1}$  from the first-order approximation  $s_t \approx 1 - a_{t-1} e^{-1/\tau}$  of  $s_t$ . Going into formula (4) we get the final model of a homogeneous random network with

$$a_{t+1} = \frac{1}{\Gamma\left(\frac{1}{K}\right)} \int_0^{\mu a_t} x^{1/K-1} e^{-x} dx \tag{5}$$

$$s_{t+1} = (1 - a_t e^{-1/\tau}) (1 - (1 - s_t) e^{-1/\tau}).$$

In contrast to (3),  $s_t$  is now interpreted as the average synaptic reliability and it explicitly depends only on the macroscopic state at time  $t - 1$ . It is model (5) which will be investigated in the next two sections.

### 3. DYNAMICS WITHOUT SYNAPTIC RELIABILITY

To get a feeling for the dynamics of the average activity we first exclude the synaptic plasticity in (5) by setting  $s_t \equiv 1$ . This reduces the model to the one-dimensional system

$$a_{t+1} = \frac{1}{\Gamma\left(\frac{1}{K}\right)} \int_0^{\mu a_t} x^{1/K-1} e^{-x} dx. \tag{6}$$

We discuss the fixed points of this one-dimensional dynamical system. Since the right-hand side of (6) has the form of a gamma-distribution function

$$F_K(y) \doteq \frac{1}{\Gamma\left(\frac{1}{K}\right)} \int_0^y x^{1/K-1} e^{-x} dx,$$

the activity  $a_{t+1}$  increases monotonically with  $a_t$ . Since  $F_K$  has only one turning-point, there exist at most three fixed points  $a_{t+1} = a_t$ . One of them is the zero-activity  $a_t = 0$ . The other possible fixed points of  $a_t$  are given by the roots of

$$\frac{Q_K(a)}{a} = \mu, \quad a \in (0, 1), \tag{7}$$

where  $Q_K(a)$  denotes the quantile of the distribution function  $F_K$  of order  $a$ . Recall that by definition the quantile  $Q_K$  is the inverse function of  $F_K$ . Given  $K$ , there exist non-trivial fixed points only if the average number  $\mu$  of connections exceeds

$$\mu_K \doteq \min_{a \in (0, 1)} \frac{Q_K(a)}{a}.$$

Since the left-hand side of (7) is a convex function of  $a$  tending to infinity for  $a \rightarrow 0$  and  $a \rightarrow 1$ , there are exactly two solutions  $a_l < a_h$  of (7) in case  $\mu > \mu_K$  and exactly one solution  $a_l = a_h$  in case  $\mu = \mu_K$ . The solutions  $a_l$  and  $a_h$  of (7) correspond to the possible intersection points of the curve  $a \rightarrow F_K(\mu a)$  with the diagonal  $a_t = a_{t+1}$  in Figure 1b. Notice that (6) may be written as  $a_{t+1} = F_K(\mu a_t)$ .

The dynamical behavior of (6) at the fixed points 0,  $a_l$  and  $a_h$  is obtained by considering the slope of the function  $a \rightarrow F_K(\mu a)$ : a fixed point is attracting if the slope therein has modulus less than 1 and repelling if the modulus is larger than 1. Using the fact that  $F_K(\mu a) < 1$  for  $a = 1$ , these slopes may be derived directly. In any case the slope at 0 is  $\leq 1$ . When  $\mu = \mu_K$ , the slope at the single non-trivial fixed point  $a_l = a_h$  is 1 since  $a \rightarrow F_K(\mu a)$  meets the diagonal tangentially there. When  $\mu > \mu_K$ , the slope at  $a_l$  is  $> 1$  while at  $a_h$  it is  $< 1$  (cf. Figure 1).

Now we assume that there is a solitary spontaneous activity  $a_{sp}$  of the network at time  $t = 0$ . The discussion on the slope of  $\phi$  at the possible fixed points leads to the following theorem.

**THEOREM 2.** *With the notations from above the dynamical behavior of (6) is classified according to*

- $\mu < \mu_K$  : extinction for any  $a_{sp} \in [0, 1]$
- $\mu = \mu_K$  : extinction for  $a_{sp} \in [0, a_l)$ ,  
convergence to  $a_l$  for  $a_{sp} \in [a_l, 1]$
- $\mu > \mu_K$  : extinction for  $a_{sp} \in [0, a_l)$ ,  
convergence to  $a_h$  for  $a_{sp} \in (a_l, 1]$ .

An analogous classification is given in Amari (1971, theorem 6) for the case that the activity  $a_{n+1}$  at time step  $n + 1$  is the cumulated Gaussian distribution of the activity  $a_n$  at time  $n$ .

To illustrate the theorem, let us choose the undamped EPSP to be  $K = 0.1$ . Recall that the threshold  $\theta$  is normalized to 1. The dynamics has a single non-trivial fixed point if and only if the average  $\mu$  of the Poisson distributed connections is  $\mu_K = 15.58$ . Setting  $\mu = 30$ , there are two non-trivial fixed points  $a_l = 0.26$  and  $a_h = 0.99$ . Figure 1 shows the function  $a_t \rightarrow a_{t+1} = F_K(\mu a_t)$  together with trajectories starting at  $a_0 = 0.26$  and 0.261. Notice that in the case  $\mu < \mu_K$  the curve does not intersect the line  $a_{t+1} = a_t$  and any trajectory will converge to 0.

### 4. DYNAMICS WITH SYNAPTIC RELIABILITY

In the following, we analyze the complete state equations (5) and involve the synaptic reliability  $s_t$ . In Section 4.1 we look for the fixed points of activity and synaptic reliability and discuss the local behavior of the dynamics near these fixed points. In Section 4.2 we consider examples of the possible global behavior while in Section 4.3 we ask for conditions implying such a global behavior. Finally, Section 4.4 gives an overall view of the behavior by considering the whole parameter space of  $(\mu, \tau)$  of possible connection

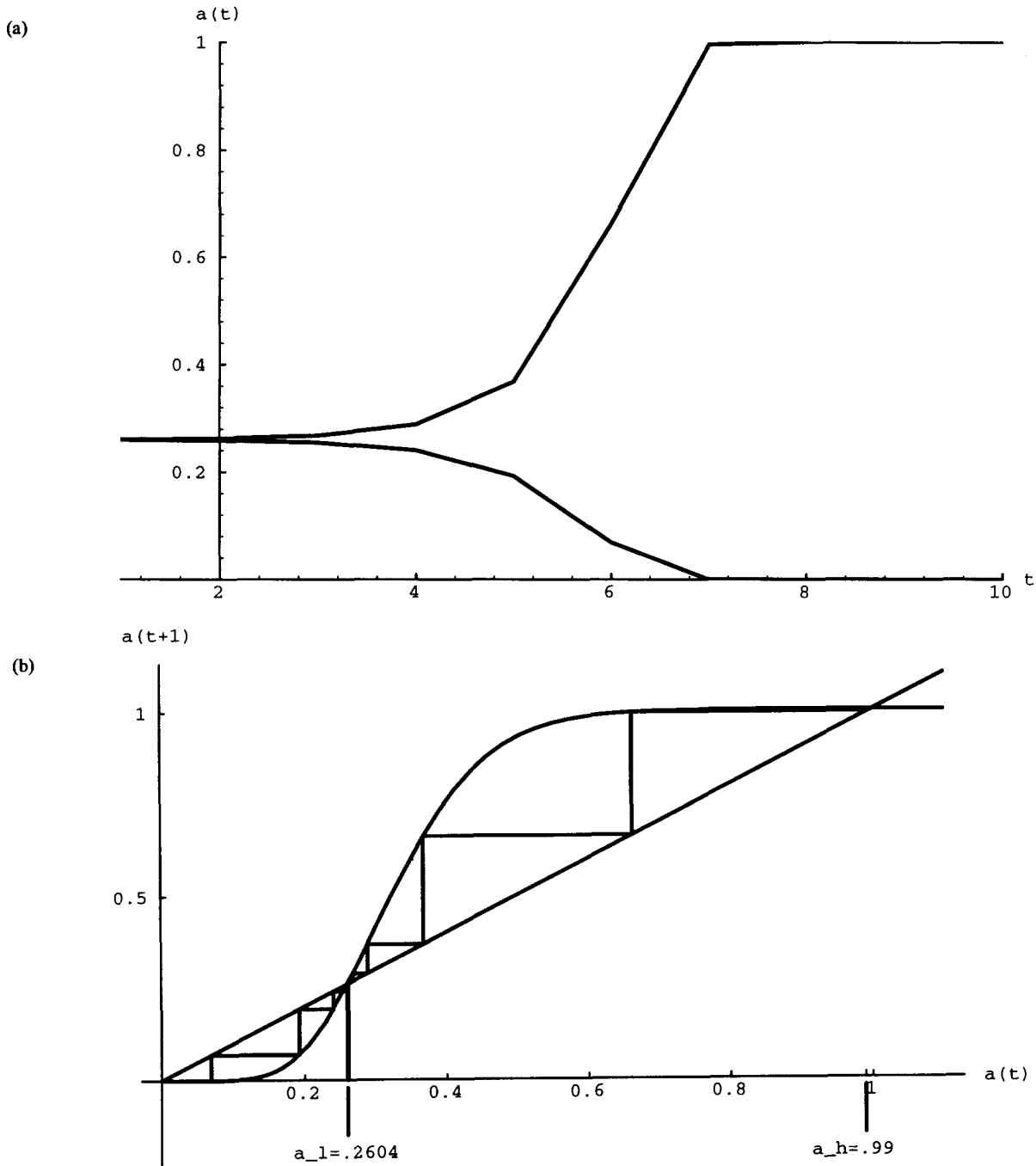


FIGURE 1. Dynamics for  $s_t \equiv 1$ . For  $K = 0.1$  and  $\mu = 30$  there exist three fixed points: the repelling fixed point  $a_l = 0.2604$  and the attracting fixed points  $0$  and  $a_h = 0.99$ . The domains of attraction are  $[0, a_l)$  and  $(a_l, 1]$ , respectively. (a) The same trajectories in the  $(t, a_t)$  diagram. All calculations were carried out using MATHEMATICA. (b) The staircase shows two trajectories starting with activities  $a_0 = 0.26$  and  $a_0 = 0.261$ .

numbers,  $\mu$ , and depression times,  $\tau$ . First, we have an empirical look at (5).

We may consider the function

$$a_t \rightarrow a_{t+1} = F_K(\mu s_t a_t) = \frac{1}{\Gamma\left(\frac{1}{K}\right)} \int_0^{\mu a_t s_t} x^{1/K-1} e^{-x} dx$$

in (5) (depicted in Figure 1 for  $s_t \equiv 1$ ) as a function

indexed by  $s_t$ . If the fluctuations of  $s_t$  are not too large, one expects that there are still the same two types of dynamical behavior as in the one-dimensional case: extinction and convergence to a non-vanishing constant activity. Indeed, this is true if the depression time  $\tau > 0$  is small (cf. Section 4.4, B). Looking at the second equality of (5), the fluctuation of  $s_t$  is restricted to the interval  $(1 - e^{-1/\tau})^2 \leq s_t \leq 1$ , which is minute when  $\tau$  is small.

However, if  $\tau$  is large,  $s_t$  may fluctuate in a large interval and two new types of dynamical behavior for  $a_t$  arise: oscillation and chaos. If, for example,  $K = 0.8$ ,  $\mu = 16$  and  $\tau = 15$ , a spontaneous activity  $a_{sp}$  of 0.05 at time  $t = 0$  is enough to provoke a stable oscillation (cf. Figure 2). Although the activity seems to die out after some steps, the network will be excited again due to the synaptic reliability which is growing in silent times.

The behavior of  $a_t$  is similar to the activity measured in slice cultures of embryonic rat spinal cord after blocking inhibitory transmission (Streit, 1993). The values of the parameters  $\tau$ ,  $K$ , and  $\mu$  were chosen to fit the range of values obtained in these experiments. To determine the synaptic depression time  $\tau$  we measured the depression at 200 ms after a stimulation of 5 Hz. From a depression of 55% we calculated the depression time to be 250 ms according to the formula  $1 - e^{-200/250} \approx 0.55$  (Streit et al., 1992). Since the synaptic delay (and thus the real time between a single time step  $t \rightarrow t + 1$  of our discrete model) is 14 ms, we have to choose  $\tau \sim 17$  to get the same depression of 0.55 ( $\approx 1 - e^{-14/17}$ ). The choice of

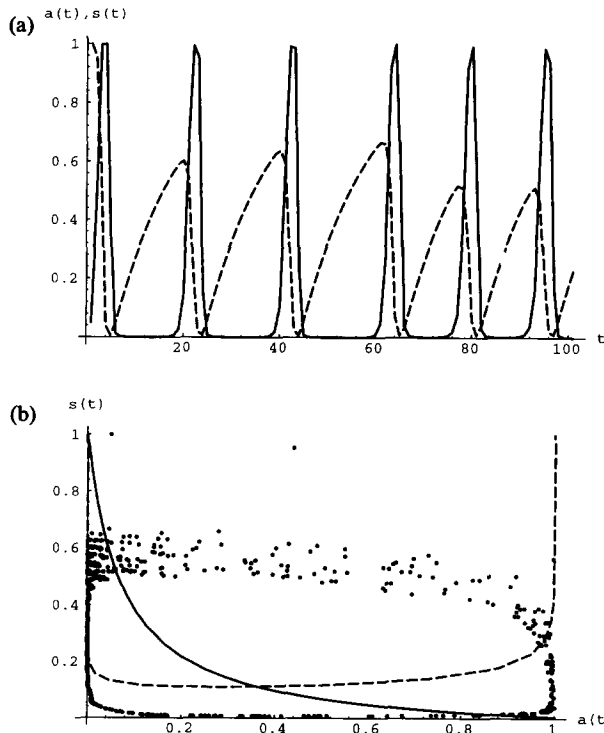


**FIGURE 2.** (a) Evolution of the activity  $a_t$  (solid) and the synaptic reliability  $s_t$  (dashed) according to the state equations (5) with a spontaneous activity  $a_{sp} = 0.05$  at time  $t = 0$ . The constants are  $K = 0.8$ ,  $\mu = 16$  and  $\tau = 15$ . If the time step in (5) is 14 ms, the activity oscillates with  $\approx 4$  Hz. This corresponds to the oscillations measured in the slice cultures which typically were about 5 Hz. (b) The points  $(a_t, s_t)$  for  $t = 0, \dots, 1000$  starting with  $(a_0, s_0) = (0.05, 1)$ . The curves  $C_{K, \mu}$  (dashed) and  $C_\tau$  (solid) are the null-clines of  $a_t$  and  $s_t$ , respectively. Their intersections correspond to the fixed points of (5).

0.8 as a mean value for the undepressed (individual) EPSP,  $K$ , relies on the fact that by exciting a single pre-synaptic cell the post-synaptic cell released an action potential in 33% of the cases while it was mute in the other cases. In absolute units the undepressed EPSP  $K$  is estimated to be  $\sim 13$  mV while the resting membrane potential and the threshold is measured to  $-56$  mV and  $-39$  mV, respectively (Streit et al., 1991). Finally, the mean number of (input-)connections  $\mu$  onto a cell is estimated to lie between 3 and 20.

#### 4.1. Local Analysis at the Fixed Point

To get a geometrical view of the dynamics, we consider the fixed points of (5) as the intersection points of two curves in the  $(a, s)$ -plane, the so-called null-clines. Let us look at (5) as a map of the phase plane  $(a, s) \in [0, 1]^2$  onto itself with the average activity  $a_t$  on the abscissa and the synaptic reliability  $s_t$  on the ordinate. The null-clines of  $a_t$  and  $s_t$  are defined by the curves in the phase plane where the values of  $a_t$  and  $s_t$ , respectively, do not change in time (Figure 2b). Abbreviating the null-cline of  $a_t$  and  $s_t$  by  $C_{K, \mu}$  and  $C_\tau$ , respectively, we have

$$\begin{aligned} C_{K, \mu} &\doteq \{(a_t, s_t) | a_t = a_{t+1} = F_K(\mu a_t s_t)\} \\ C_\tau &\doteq \{(a_t, s_t) | s_t = s_{t+1} \\ &= (1 - a_t \varepsilon_\tau)(1 - (1 - s_t) \varepsilon_\tau)\}, \varepsilon_\tau \doteq e^{-1/\tau} \end{aligned} \quad (8)$$

where  $C_{K, \mu}$  and  $C_\tau$  depend only on  $K$ ,  $\mu$  and  $\tau$ , respectively (see Figure 2). A point on  $C_{K, \mu}$  is moved by the dynamics (5) vertically while a point on  $C_\tau$  is moved horizontally. Notice that the curves may be calculated explicitly as a function of  $a_t$ . As a result one gets

$$C_{K, \mu} = \left\{ \left( a, \frac{Q_K(a)}{\mu a} \right) | a \in (0, 1) \right\}$$

and

$$C_\tau = \left\{ \left( a, \frac{(1 - \varepsilon_\tau)(1 - a \varepsilon_\tau)}{1 - \varepsilon_\tau(1 - a \varepsilon_\tau)} \right) | a \in [0, 1] \right\}.$$

The two fixed points  $a_l$  and  $a_h$  of the one-dimensional system with  $s_t \equiv 1$  may be recovered in the  $(a_t, s_t)$  diagram as the intersection points of  $C_{K, \mu}$  and  $C_0 \doteq \{(a, 1) | a \in [0, 1]\}$ . Now, the two non-trivial fixed points of the two-dimensional system are given by the intersection points of  $C_{K, \mu}$  and  $C_\tau$ . For typical values of  $K$ ,  $\mu$  and  $\tau$  the first intersection point is repelling and close to  $(a = 0, s = 1)$ . We concentrate on the second intersection point which we denote by  $P_{\text{fix}} = (a_\infty, s_\infty)$  (provided the two curves intersect).

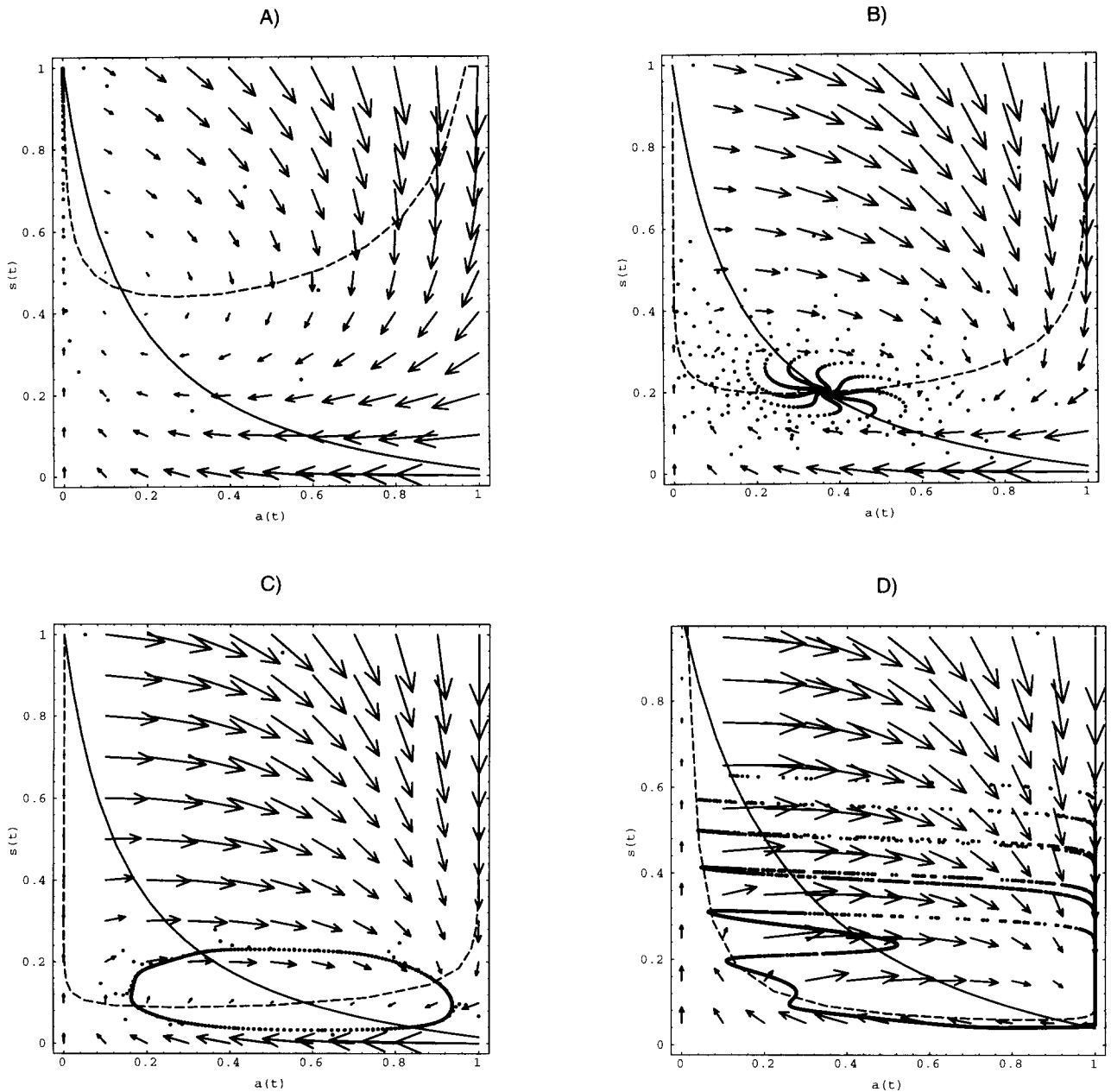


**FIGURE 3.** The four types of qualitative behavior: extinction (A), convergence to a constant activity (B), oscillation (C) and chaos (D) as described in the text. The arrows (scaled by a factor  $\frac{1}{2}$ ) illustrate the dynamics of the equations (5). Starting at  $(a_0, s_0) = (0.05, 1)$  we iterated the state equations (A) 100, (B) 700, (C) 1000, (D) 10,000 times. For the parameter values of  $K, \mu,$  and  $\tau$  see Section 4.2.

(A) *A stability criterion.* In order to analyze the local behavior of (5) at the fixed point  $P_{\text{fix}}$  we first calculate its linearization. Abbreviating

$$f_K(y) \doteq \frac{1}{\Gamma\left(\frac{1}{K}\right)} y^{1/K-1} e^{-y}$$

and

$$\varepsilon_\tau \doteq e^{-1/\tau}$$

one obtains from (5)

$$\frac{\partial(a_{t+1}, s_{t+1})}{\partial(a_t, s_t)} = \begin{pmatrix} \mu s_t f_K(\mu a_t s_t), & \mu a_t f_K(\mu a_t s_t) \\ -\varepsilon_\tau (1 - (1 - s_t)\varepsilon_\tau), & \varepsilon_\tau (1 - a_t \varepsilon_\tau) \end{pmatrix}. \tag{9}$$

According to the theorem of Hartman–Grobman [see, for example, Guckenheimer and Holmes (1990)] the system (5) is locally stable or unstable at  $P_{\text{fix}}$  if the eigenvalues  $\lambda$  and  $\lambda$  of the linearization (9) at  $P_{\text{fix}}$  have modulus  $< 1$  or  $> 1$ , respectively. Now, the

calculation of  $|\lambda|^2$  may be reduced to the calculation of the determinant as follows: consider the vector field near the fixed point  $P_{\text{fix}}$  in Figure 3. By definition, the vectors lie horizontally at the curve  $C_\tau$ . Since

$$\frac{\partial s_{t+1}}{\partial a_t} < 0,$$

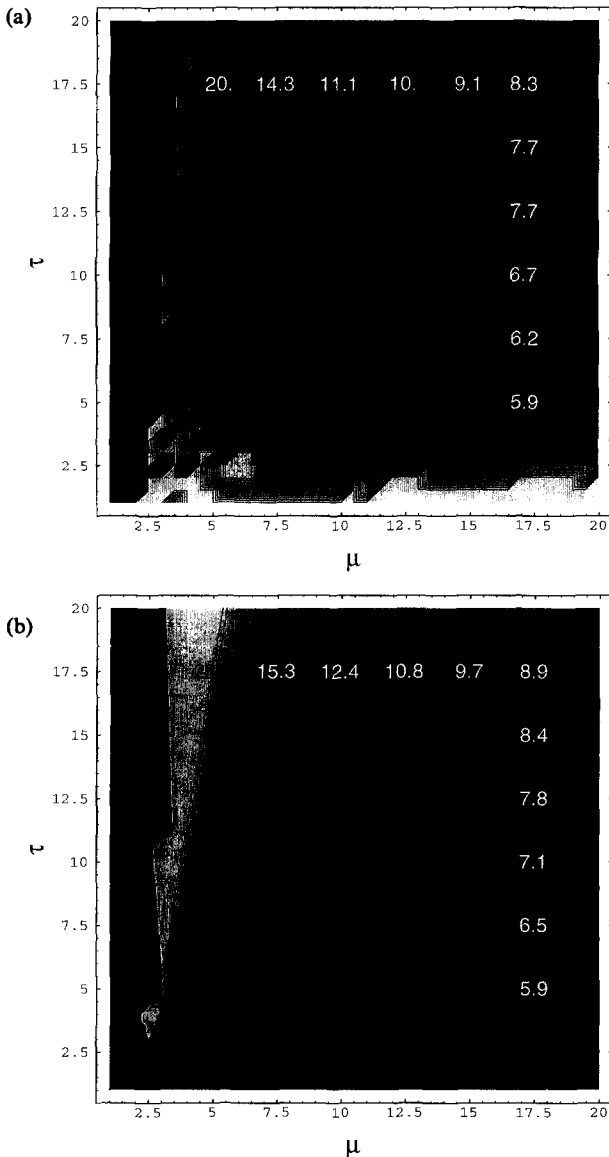


**FIGURE 4.** (a) A contour plot of the numerically exact cycle length of (5). This cycle length is identified with the average time between two neighboring relative maxima of activity  $a_t$  within the time interval  $t = 1, \dots, 100$ . The starting  $(a_1, s_1)$  was chosen near  $(\approx 0.001)P_{\text{fix}}$ . (b) The cycle length  $L_{0.8}(\mu, \lambda)$  of the linearization (9) at  $P_{\text{fix}}$ . For the definition of  $L_K(\mu, \lambda)$  see Section 4.1 (B). A comparison between the “real” cycle length and the calculated one gave, in general, an underestimate of the former by less than 20% within the domain  $5 < \mu, \tau \leq 20$ . The deviation was larger at the eight singular black regions within this domain. Again, the time step of our discrete model corresponds to a biological time of 14 ms.

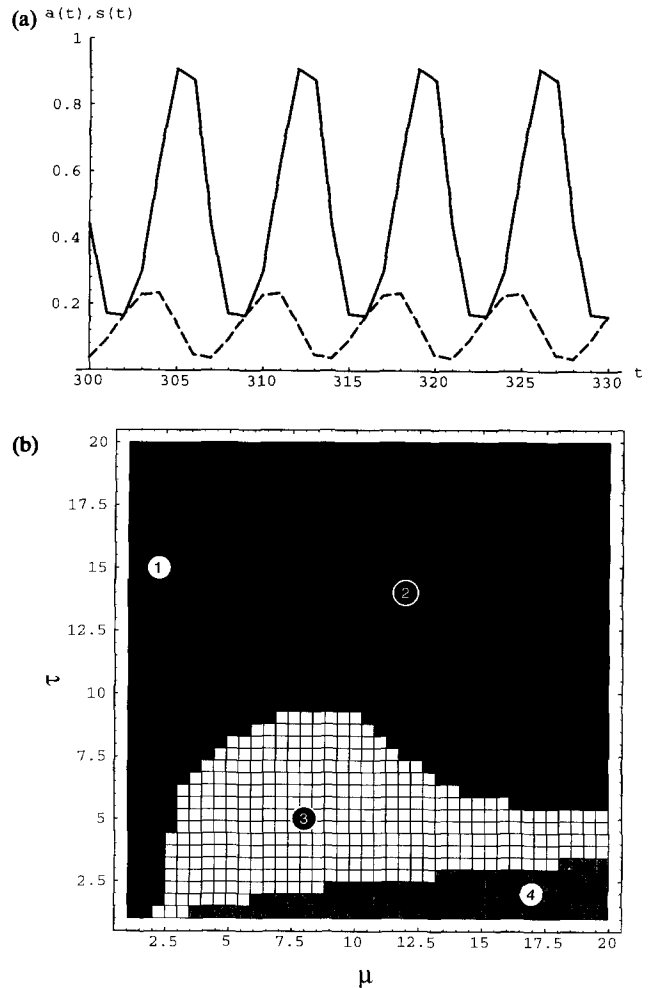


**FIGURE 5.** (a) A strictly periodic repetition of activity  $a_t$  with only seven activity levels ( $K = 0.8$ ,  $\tau = 8$ , and  $\mu = 19$ ). The parameter value for  $\mu$  is found with the help of Figure 6a. The dashed line represents the synaptic reliability  $s_t$ . (b) The regions of extinction (1), local stability (3 and 4), local instability (2) and of global stability (4). Region (1) shows the parameter values  $(\mu, \tau)$  satisfying condition (10) for extinction, regions (2) and (3) distinguish between  $|\lambda| > 1$  and  $|\lambda| < 1$  (lemma 3) and region (4) shows the parameter values satisfying the conditions of Theorem 5. Recall that the unit of  $\tau$  corresponds to 14 ms. Cf. text Section 4.4.

the arrows turn right and they necessarily change their sign at the intersection point  $P_{\text{fix}}$  of the two nullclines  $C_{K,\mu}$  and  $C_\tau$ . Since

$$\frac{\partial^2 s_{t+1}}{\partial a_t \partial s_t} = -\varepsilon \frac{2}{\tau} < 0,$$

the speed of rotation is bounded away from 0 and thus survives the linearization at the fixed point. Therefore, the linearization (9) at  $P_{\text{fix}}$  is composed either of a genuine rotation or of a shearing. In the first case, the eigenvalues  $\lambda$  and  $\bar{\lambda}$  are complex-valued and conjugated while in the second case there is a single non-vanishing eigenvalue  $\lambda$  of multiplicity 2. In both cases, the squared modulus of the eigenvalue(s)

is given by the determinant of (9) at  $P_{\text{fix}}$  and we obtain:

LEMMA 3. *The system (5) is locally stable (unstable) at the fixed point  $P_{\text{fix}} = (a_{\infty}, s_{\infty})$  if*

$$|\lambda|^2 = \det \frac{\partial(a_{t+1}, s_{t+1})}{\partial(a_t, s_t)} \Big|_{P_{\text{fix}}} = \mu \varepsilon_{\tau} f_K(\mu a_{\infty}, s_{\infty})(s_{\infty} + a_{\infty}(1 - \varepsilon_{\tau})) < 1 (> 1).$$

(B) *Estimate of Cycle Length.* Next we are interested in the cycle length of a possible oscillation of  $a_t$ . At first-order approximation of the activity cycle length is given by the rotation part of the linearization (9) at  $P_{\text{fix}}$ . Let us write the eigenvalue  $\lambda$  in the form  $\lambda = |\lambda|e^{2\pi i\varphi}$  and suppose  $0 < \varphi \leq 1$ . Then the cycle length of the linearization at  $P_{\text{fix}}$  is given by

$$L_K(\mu, \tau) \doteq \frac{1}{\varphi}.$$

Numerical investigations show that this is not only locally a good estimate of the activity cycle length, but even *globally*. Figure 4a represents the average cycle length of (5) averaged between  $t = 1, \dots, 100$  and starting near  $P_{\text{fix}}$ . The right side represents the cycle length  $L_{0.8}(\mu, \tau)$  of the linearization at  $P_{\text{fix}}$ . A dark region, right, corresponds to a small value, while a light region corresponds to a larger value. In the example of Figure 5a, one calculates  $L_{0.8}(19, 8) = 6.5$  compared with the numerically exact cycle length of 7.0. Comparison of  $L_{0.8}(\mu, \tau)$  with the averaged cycle length showed that the approximation error in general is less than 20% if  $\mu$  and  $\tau$  are larger than 5 (we tested up to  $\mu, \tau \leq 20$ ). Looking at Figure 4 one asserts that  $L_{0.8}(\mu, \tau)$  is growing if  $\tau/\mu$  is growing. This supports the intuition that the real cycle length of activity should be large when  $\tau$  is large or  $\mu$  is small.

What can be proved in any case by a simple phase-plane consideration is:

LEMMA 4. *For any  $K, \mu, \tau > 0$  with existing fixed point  $P_{\text{fix}}$  the cycle length of activity is  $\geq 4$ . In particular, the cycle length  $L_K(\mu, \tau)$  of the linearization at  $P_{\text{fix}}$  is  $\geq 4$ .*

The lemma follows from the fact that by the curves  $C_{K,\mu}$  and  $C_{\tau}$  there is a subdivision of the space  $(a_t, s_t) \in [0, 1]^2$  into four domains with intersection point  $P_{\text{fix}}$ . Any cycle  $(a_t, s_t), (a_{t+1}, s_{t+1}), \dots$  runs in a clockwise direction around  $P_{\text{fix}}$  without skipping any of the four domains. [This may be shown by considering the images of  $C_{K,\mu}$  and  $C_{\tau}$  under the mapping (5) and using some monotonicity properties of (5).]

(C) *Hopf Bifurcation.* Although the lemma gives an estimate of the cycle length which is far away from the local estimate  $L_K(\mu, \tau)$ , it yields a necessary condition for Hopf bifurcation. The Hopf bifurcation describes the phenomenon that, for example, by varying the parameter  $\mu$ , an attracting fixed point  $P_{\text{fix}}$  changes into a repelling one together with an attracting limit cycle around it. Lemma 4 guarantees that when  $|\lambda| = 1$ , it follows  $\lambda^k \neq 1$  for  $k = 1, 2$ , and 3. A further condition that Hopf bifurcation takes place at some values  $K, \mu$ , and  $\tau$  with  $|\lambda(K, \mu, \tau)| = 1$  is that the eigenvalue  $\lambda$  transverses, with non-vanishing speed, the unit-circle, i.e.,

$$\frac{\partial|\lambda|}{\partial\mu} \neq 0$$

at  $|\lambda| = 1$ . For an exact formulation of the bifurcation phenomenon for diffeomorphism see Marsden and McCracken (1976, theorem 6.2). An example of Hopf bifurcation is given by (B)–(C) in the following subsection.

#### 4.2. Examples of the four Types of Qualitative Behavior

We discuss four numerical examples showing the possible behavior of model (5) by varying the

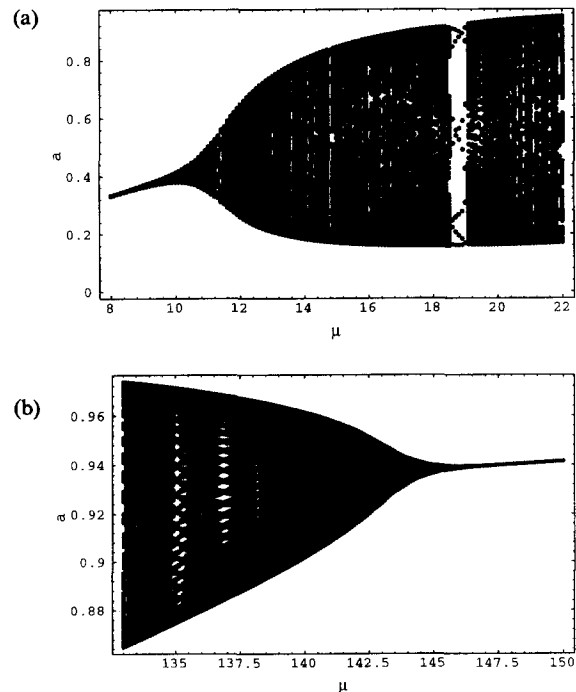


FIGURE 6. Two regions of the bifurcation diagram. Starting with  $(a_0, s_0) = (0.05, 1)$  we plotted  $a_t, t = 800, \dots, 1000$ , against  $\mu$ . The parameters  $K = 0.8$  and  $\tau = 8$  are kept fixed. Note the different scales on the vertical axes for  $a_t$ . For  $\mu = 19$  a strictly periodic oscillation occurs (cf. Figure 5). The convergence of the activity for high values of  $\mu$  is predicted by Theorem 6.

undepressed EPSP,  $K$ , the average number of connections,  $\mu$ , and the synaptic depression time,  $\tau$ . We refer to Figs 3 and 5 where the arrows represent the differences  $(a_{t+1}, s_{t+1}) - (a_t, s_t)$  defined at the various points  $(a_t, s_t)$  and scaled with a factor  $\frac{1}{5}$ .

(A) *Extinction.* The undamped EPSP is chosen to be  $K = 0.8$ , the synaptic depression time is  $\tau = 8$  and the mean of the Poisson distributed connections is  $\mu = 4$ . According to lemma 3 the fix-point  $P_{\text{fix}}$  is calculated to be repelling ( $|\lambda| = 1.01$ ). Starting at  $(a_0, s_0) = (0.14, 0.46)$  leads to extinction after 50 time steps although the starting point is near  $P_{\text{fix}}$ . In particular, no attracting limit cycle seems to occur when the fixed point  $P_{\text{fix}}$  changes from an attracting ( $\mu = 5$ ) into a repelling one ( $\mu = 4$ ).

(B) *Constant Activity.* The same parameter values as in (A) but with  $\mu = 9$ . The fixed point  $P_{\text{fix}}$  is now attracting ( $|\lambda| = 0.99$ ) and a solitary spontaneous activity  $a_{\text{sp}} = 0.05$  at  $t = 0$  (with  $s_0 = 1$ ) is enough to maintain a limit activity  $a_t \xrightarrow{t \rightarrow \infty} a_{\text{fix}} = 0.37$ .

(C) *Oscillation.* The same parameter values as in (A) and (B), but with  $\mu = 20$  and modulus  $|\lambda| = 1.03$  of the eigenvalue at  $P_{\text{fix}}$ . At  $\mu = 11.3$  Hopf bifurcation occurs: the stable fixed point  $P_{\text{fix}}$  changes into an unstable fixed point and an attracting limit cycle arises. The limit cycle is growing with  $\mu$  until  $\mu \approx 25$  where the activity  $a_t$  oscillates between 0.18 and 0.96 (cf. Figure 6). Increasing  $\mu$  further, the attracting limit cycle shrinks slowly until it collapses at  $\mu \approx 143$  to the fixed point  $P_{\text{fix}}$ . The existence of a limit cycle leads to another kind of stability result for the fixed point  $P_{\text{fix}}$ : if the trajectory starts at some point  $(a_0, s_0)$  lying within the limit cycle, it remains there for all times  $t \geq 0$ . This statement follows from a simple topological argument relying on the continuity of the mapping  $(a_t, s_t) \rightarrow (a_{t+1}, s_{t+1})$ .

(D) *Chaos.* Chaotic behavior (cf. Figure 3) seems to occur only if the undamped EPSP,  $K$ , is small. In our example we chose  $K = 0.1$ ,  $\tau = 5$ ,  $\mu = 268.66$  and as starting values again  $(a_0, s_0) = (0.05, 1)$ . The dynamics are chaotic in the sense that they are not predictable whether the cycle in the  $(a_t, s_t)$  diagram makes an upper or lower turn. The necessary reduction of the undamped EPSP  $K$  has an experimental analogy: random patterns of activity are found in the spinal cord cultures in the presence of inhibitory synaptic transmission. This situation corresponds to a network with low synaptic weights ( $K \leq 0.1$ ) in the model (cf. Figure 3, D).

### 4.3. Conditions Guaranteeing the Amplification, Survival or Extinction of a Spontaneous Activity

In the following, we present three criteria for different long-term behavior of the network activity. We ask for the critical amount of a solitary spontaneous

activity  $a_{\text{sp}}$  at time  $t = 0$  which is needed to lead (A) to non-vanishing activity at least in the next time step (B) to non-vanishing activity for any of the following time steps and (C) to extinction.

Let us fix the parameter values  $K, \mu, \tau$  and suppose that

$$\mu > \mu_K = \min_{a \in (0,1)} \frac{Q_K(a)}{a}.$$

Recall that  $a_l < a_r$  denote the two non-vanishing fixed points of the activity  $a_t$  in case  $s_t \equiv 1$  and  $\mu > \mu_K$ .

(A) *Condition for Amplification.* First we give a condition that the network gets excited at least once after a spontaneous activity, i.e., that  $a_1 > a_0 = a_{\text{sp}}$ . Since at time  $t = 0$  the synaptic reliability is 1, the activity  $a_1$  may be calculated according to (6). As the analysis of the one-dimensional system shows (cf. Theorem 2), the equality  $a_1 > a_{\text{sp}}$  is true if and only if  $a_l < a_{\text{sp}} < a_h$ . But this last condition is equivalent to

$$\frac{Q_K(a_{\text{sp}})}{a_{\text{sp}}} < \mu$$

due to the convexity of the left-hand side of (7). In other words, the activity  $a_t$  is growing temporarily after spontaneous activity  $a_{\text{sp}}$  if and only if

$$\frac{Q_K(a_{\text{sp}})}{a_{\text{sp}}} < \mu.$$

(B) *Condition for Survival.* In order to guarantee the survival of the activity, say  $a_t > a_l$  for all  $t > 0$ , we have to impose an additional condition on the synaptic depression time  $\tau$ . Considering the dynamics shown in the  $(a_t, s_t)$  diagram together with the vector field of (5), it is easy to see that  $a_t > a_l$  for any  $t > 0$  if the curve  $C_\tau$  lies above

$$\min\{s | (a, s) \in C_{K, \mu}\} = \frac{\mu_K}{\mu}.$$

Recall that  $(a_l, 1)$  is the first intersection point of  $C_{K, \mu}$  with  $s_t \equiv 1$ . Since the curve  $C_\tau$  is monotonically decreasing in  $a$ , its minimal  $s$ -value is reached at  $a = 1$  and it is given by

$$\min\{s | (a, s) \in C_\tau\} = \frac{(1 - \varepsilon_\tau)^2}{1 - \varepsilon_\tau(1 - \varepsilon_\tau)}.$$

This global result is summarized by:

**THEOREM 5.** *Let the dynamic (5) start with a solitary*

spontaneous activity  $a_{sp} > 0$  and a synaptic reliability  $s_0 = 1$ . If the positive parameters  $K$ ,  $\mu$  and  $\tau$  satisfy

$$(a) \frac{Q_K(a_{sp})}{a_{sp}} < \mu \quad \text{and} \quad (b) \frac{\mu K}{\mu} < \frac{(1 - \epsilon_\tau)^2}{1 - \epsilon_\tau(1 - \epsilon_\tau)}$$

then for any  $t \geq 0$  the activity  $a_t$  is larger than  $a_l > 0$  and thus will never die out.

Instead of condition (a) the condition  $a_{sp} > a_l (> 0)$  may be required as well. Notice the condition (b) will be satisfied if  $\mu$  is large and/or  $\tau$  is small.

To illustrate the theorem we come back to the example in Section 3 with  $K = 0.1$  and  $\mu = 30$ . Theorem 2 states that in the case of constant synaptic reliability  $s_i \equiv 1$  a solitary spontaneous activity of  $a_{sp} > a_l = 0.26$  will lead to a limit activity of  $\lim_{t \rightarrow \infty} a_t = a_h = 0.99$ . Theorem 5 now states that in the case of variable synaptic reliability the same spontaneous activity guarantees an activity  $a_t > 0.26$  for any  $t \geq 0$  provided the synaptic depression time  $\tau$  is less than 1.0.

(C) Condition for Extinction. Finally, we mention that any spontaneous activity eventually leads to extinction if the curve  $C_\tau$  lies below from  $C_{K, \mu}$  and thus no fixed point  $P_{fix}$  may exist. Algebraically this condition is given by

$$\frac{Q_K(a)}{\mu a} > \frac{(1 - \epsilon_\tau)(1 - a\epsilon_\tau)}{1 - \epsilon_\tau(1 - a\epsilon_\tau)}, \text{ for all } a \in (0, 1). \quad (10)$$

In contrast to Theorem 5 this condition for extinction is satisfied if  $\mu$  is small and/or  $\tau$  is large. The extinction follows from the fact that the curve  $C_\tau$  is attracting for any starting point  $(a_0, s_0) \in [0, 1]^2$  while the vertical line  $a_t \equiv 0$  is attracting for any starting point lying below from  $C_{K, \mu}$ . If, for example,  $K = 0.8$  and  $\tau = 8$  the inequality is satisfied for any  $\mu$  less than the critical value

$$\mu_0 = \min_{a \in (0, 1)} \frac{Q_K(a)}{a} \frac{1 - \epsilon_\tau(1 - a\epsilon_\tau)}{(1 - \epsilon_\tau)(1 - a\epsilon_\tau)} = 2.83$$

(cf. Figure 5b).

**4.4. The Qualitative Behavior as a Function of  $\mu$  and  $\tau$**

We are interested in the long-term behavior of the network activity  $a_t$  in dependence of the average number of connections,  $\mu$ , and of the synaptic depression time,  $\tau$ . To get an overview, we determined the local behavior at  $P_{fix}$  for a matrix of  $(\mu, \tau)$  values. Fixing the undamped EPSP to  $K = 0.8$ , we calculated the modulus  $|\lambda|$  of the eigenvalue  $\lambda$  according to lemma 3. Figure 5b shows four different regions:

- Black with  $|\lambda| > 1$  and a repelling fixed point  $P_{fix}$ . Here, either oscillation or extinction takes place.
- White or light-gray with  $|\lambda| < 1$  and an attracting fixed point  $P_{fix}$ . The activity typically either converges to a non-zero limit activity  $a_{fix}$  or, depending on the initial values, dies out.
- Dark-gray without any fixed point and thus extinction in any case according to Section 4.3 (C).
- Light-gray where the global stability conditions of Theorem 5 are satisfied with a starting activity of  $a_{sp} = 0.05$ .

(A) Dependence on the Average Number  $\mu$  of Connections. Let us focus to the horizontal line  $\tau \equiv 8$ . The numerical examples (A)–(C) of Section 4.2 illustrate the dynamical behavior when  $\mu$  is increased from  $\mu = 4$  to 9 and 20. The local behavior at  $P_{fix}$  changes from instability to stability and returns to instability again (cf. Figure 3). This is rather striking since one expects that once  $P_{fix}$  is stable, an increment of  $\mu$  would increase the limit activity  $a_{fix}$  only rather than destabilize  $P_{fix}$ . Indeed, this is the case if  $\mu$  is large. From lemma 3 one deduces the following:

**THEOREM 6.** *Given  $K, \tau > 0$ , there exists  $\mu_1 > 0$ , such that for any  $\mu > \mu_1$  the fixed point  $P_{fix} = (a_\infty, s_\infty)$  of (5) exists and is stable. Moreover, the limit activity  $a_\infty$  converges to 1 for  $\mu \rightarrow \infty$ .*

*Proof.* We have to show that  $|\lambda|^2 = \mu\epsilon_\tau f_K(\mu a_\infty s_\infty)(s_\infty + a_\infty(1 - \epsilon_\tau)) < 1$  for  $\mu$  large enough. Considering the representation of  $C_\tau$  and  $C_{K, \mu}$  as a function of  $a_t$  we conclude that for the coordinates  $a_\infty$  and  $s_\infty$  of the intersection point  $P_{fix}$  one has  $a_\infty \rightarrow 1$  and

$$s_\infty \rightarrow \frac{(1 - \epsilon_\tau)^2}{1 - \epsilon_\tau(1 - \epsilon_\tau)} > 0$$

for  $\mu \rightarrow \infty$ . (Here we need that, due to the formula  $a = F_K(\mu a s)$ , for any  $a \in (0, 1)$ , the unique point  $(a, s_\mu(a)) \in C_{K, \mu}$  converges to  $(a, 0)$  for  $\mu \rightarrow \infty$  and that  $C_\tau$  does not depend on  $\mu$ .) In particular,  $a_\infty$  and  $s_\infty$  are bounded from below. Due to the properties of  $f_K$ , the function  $\mu \rightarrow f_K(\mu a_\infty, s_\infty)$  therefore is decreasing exponentially for large  $\mu$  and the desired inequality  $|\lambda|^2 < 1$  for  $\mu$  large enough is established. □

In our example with  $K = 0.8$  and  $\tau = 8$  the value  $\mu_1$  where  $P_{fix}$  changes definitely from a repelling to an attracting fixed point is found to be  $\mu_1 \approx 143$ . For this value of  $\mu$  the limit activity  $a_\infty$  is about 0.94 (cf. Figure 6). Recall that on the other hand, any activity will lead to extinction if  $\mu < \mu_0 = 2.83$ .

In order to get an impression of what happens when  $\mu$  is increased we take two regions of the  $(\mu, a)$ -bifurcation diagram (Figure 6). For each

value of  $\mu$  a diagram shows the activities  $a_t$  for  $t = 700 \dots 1000$  after starting at  $(a_0, s_0) = (0.05, 1)$ . Notice that a continuous interval of  $a_t$  values does not imply chaos: the activity  $a_t$  typically is oscillating with a constant frequency. However, if there is only a finite number of activity levels  $a_t$ , the oscillation is strictly periodic (cf. Figure 5a).

(B) *Dependence on the Synaptic Depression Time  $\tau$* . Focusing on a vertical line  $\mu \equiv \text{const}$ , the converse statements hold: If  $\tau$  is large enough to satisfy (10), any activity dies out, independently of the spontaneous activity  $a_{sp}$  at the starting time. In turn, if  $\tau$  is small enough (and  $\mu > \mu_K$ ) the fixed point  $P_{\text{fix}} = (a_\infty, s_\infty)$  exists and is stable. For  $\tau \rightarrow 0$  the limit activity  $a_\infty$  tends to the stable limit activity  $a_h$  of the one-dimensional system with  $s_t \equiv 1$ .

### 5. CONCLUSIONS

The main finding of our investigation is the fact that, within a broad range of biologically motivated parameters, oscillations in an “embryo typic” network occur. In contrast to the frequently made assumption on oscillation generating networks, we are starting out from

- a single random network with *equally* distributed connections and
- purely *excitatory* synaptic connections between the neurons.

In particular, to provoke rhythmic activity, no subpopulation of inhibitory cells is required [as is considered in Amari (1971)] if the cells have only depression-like properties. Moreover, no structured connectivity is needed to produce stable oscillations as is often assumed in pattern generators (see, for example, Getting (1988)).

Our model may give a partial answer to the fundamental question raised in Vibert et al. (1994, p. 589) as to whether biological rhythms are driven by pacemaker cells or not. The close agreement with the experiment supports the conjecture that in the slice culture of embryonic rat spinal cord, rhythmic activity is an emerging property of the network and that pacemakers are not required.

The finding that stable oscillations naturally arise in unstructured networks with “embryonic properties” may be ontogenetically relevant. Rhythmic patterns of such spinal cord networks in the embryogenetic stage play an important role in the formation of specific architectures of pattern generators or other cell assemblies.

### REFERENCES

Amari, S.-I. (1971). Characteristics of randomly connected

threshold-element networks and network systems. *Proceedings of the IEEE*, **59**(1), 35–47.

Anninos, P. A., Beek, B., Csermely, T. J., Harth, E. M., & Pertile, G. (1970). Dynamics of neural structures. *Journal of Theoretical Biology*, **26**, 121–148.

Fournou, E., Argyrakakis, P., & Anninos, P. A. (1993). Neural nets with markers and Gaussian-distributed connectivities. *Connection Science*, **5**(1) 77–94.

Getting, P. (1988). Comparative analysis of invertebrate central pattern generators. In A. Cohen, S. Rosignol, & S. Grillner, (Eds.) *Neural control of rhythmic movements in vertebrates*, (Chapter 4, pp. 101–128). New York: John Wiley.

Grillner, S. (1985). Neurobiological bases of rhythmic motor acts in vertebrates. *Science*, **228**, 143–149.

Guckenheimer, J., & Holmes, P. (1990). *Nonlinear oscillation, dynamical systems, and bifurcations of vector fields* (3rd ed.). Berlin: Springer.

Marsden, J. E., & McCracken, M. (1976). *The Hopf bifurcation and its applications*. New York: Springer.

O'Donovan, M., Sernagor, E., Sholomenko, G., Ho, S., Antal, M., & Yee, W. (1992). Development of spinal motor networks in the chick embryo. *Journal of Experimental Zoology*, **261**, 261–273.

Oppenheim, R. W. (1975). The role of supraspinal input in embryonic motility: A reexamination in the chick. *Journal of Computational Neurology*, **160**, 37–50.

Streit, J. (1993). Regular oscillations of synaptic activity in spinal networks in vitro. *Journal of Neurophysiology*, **70**, 871–878.

Streit, J., Spenger, C., & Lüscher, H.-R. (1991). An organotypic spinal cord-dorsal root ganglia-skeletal muscle coculture of embryonic rat. II. Functional evidence for the formation of spinal reflex arcs in vitro. *European Journal of Neuroscience*, **3**, 1054–1068.

Streit, J., Lüscher, C., & Lüscher, H.-R. (1992). Depression of postsynaptic potentials by high-frequency stimulation in embryonic motoneurons grown in spinal cord slice cultures. *Journal of Neurophysiology*, **68**(5), 1793–1803.

Vibert, J.-F., Pakdaman, K., & Azmy, N. (1994). Interneural delay modification synchronizes biologically plausible neural networks. *Neural Networks*, **7**(4), 589–607.

### NOMENCLATURE

$t$	discrete time (in units of 14 ms)
$\mu$	average number of connections
$K$	average undepressed post-synaptic potential (in units of 13 mV)
$\tau$	synaptic depression time (in units of 14 ms)
$a_t$	average activity
$s_t$	average synaptic efficacy (or reliability)
$a_t^i$	activity of $i$ th neuron
$s_t^i$	synaptic efficacy of $i$ th neuron
$\eta_i$	critical number of depressed EPSPs
$\mu_K$	critical number of connections for non-trivial fixed points
$a_l, a_h$	fixed points for $s_t \equiv 1$
$a_{sp}$	initial spontaneous activity of network
$C_{K, \mu}$	null-cline of $a_t$
$C_\tau$	null-cline of $s_t$
$P_{\text{fix}}$	intersection point of $C_{K, \mu}$
$(a_\infty, s_\infty)$	coordinates of $P_{\text{fix}}$
$\varepsilon_\tau$	$\varepsilon_\tau \doteq e^{-1/\tau}$

$L_K(\mu, \tau)$  cycle length of linearization (9) at  $P_{\text{fix}}$   
 $f_K(\cdot)$  density function of gamma-distribution  
 $F_K(\cdot)$  gamma-distribution function

$Q_K(\cdot)$  quantile of  $F_K(\cdot)$ , ( $Q_K = F_K^{-1}$ )  
 $\langle \cdot \rangle$  expectation value